15 August 1994

OPTICS COMMUNICATIONS

ELSEVIER

Optics Communications 110 (1994) 410–424

Full length article

A novel waveguide Mach–Zehnder interferometer based on multimode interference phenomena

R.M. Jenkins, R.W.J. Devereux, J.M. Heaton

Defence Research Agency, Electronics Division, St Andrews Road, Malvern, Worcestershire, WR14 3PS, UK

Received 13 April 1992; revised manuscript received 30 November 1992

Abstract

A novel form of Mach–Zehnder interferometer based on multimode interference (MMI) phenomena in multimode waveguides is predicted and demonstrated. The interferometer is based on symmetrically feeding fundamental mode fields from two square waveguides, $2a \times 2a$, in cross section, into a multimode rectangular guide, $2a \times 2b$, $(b > a)$. As a result of multimode interference phenomena, depending on whether the input fields are "in" or "out of" phase, two completely different forms of resultant field pattern are produced at a distance of $2b^2/\lambda_c$, along the multimode guide. The predictions are verified experimentally at 10.6 μm with hollow dielectric guides, but the underlying design concepts are considered to be much more broadly applicable.

1. Introduction

Rivlin et al. [1] predicted interesting transmission properties for coherent light in multimode waveguides and demonstrated that multiple images of an illuminated slit could be produced by a suitable choice of guide geometry. Bryngdahl [2] suggested that multimode waveguides might be used to create both single and multiple self-images of symmetric objects illuminated with coherent or incoherent light. Ulrich [3] explained the formation of single self-images in terms of the superposition of harmonic modes and demonstrated single order self-imaging of a coherently illuminated slit in a planar liquid guide. Ulrich and Ankele [4] described the formation of multiple self-images ray optically and demonstrated double order self-imaging again with a liquid guide. Although Ulrich et al. [3,4] undertook their experiments with symmetric images their theoretical work assumed the more general case of asymmetric images which resulted in the excitation of both symmetric and antisymmetric waveguide modes. They predicted that an N-fold replication of an image in the input plane of a multimode waveguide would be achieved at a guide length of $4(2b)^2/N\lambda_c$, for a planar guide of width, $2b$, where λ_c was the wavelength of a plane wave in the core.

Based on earlier studies of multimode interference phenomena in circular cross sectioned waveguides [5], we have proposed and demonstrated, symmetrically fed rectangular guides as the basis of fundamental mode beam splitters [6–9]. These provide a function similar to a cascade of "Y" junctions but have advantages in terms of length, efficiency and ease of manufacture. In such splitters a square sectioned waveguide, $2a \times 2a$, carries a fundamental mode field symmetrically into a multimode rectangular guide, $2a \times 2b$. Because of the symmetric form of this type of multimode interference (MMI) splitter, it relies solely on the excitation and propagation of symmetric modes. Numerical field calculations [6–9] supported by a modal analysis [10], have shown that in

SSDI 0030-4018(94)00174-S

such configurations, the waveguide length required to achieve an N-way fundamental mode replication is given as $(2b)^2/N\lambda_c$. This guide length is one quarter of that predicted for the same order of splitting in mixed mode (symmetric plus antisymmetric mode) splitters; as a result symmetric mode splitters should have advantages in both manufacture and use. A 1-to-2-way splitter has been demonstrated with hollow dielectric guides and 10.6 μm radiation [8] and a 1-to-20-way splitter with GaAs ribbed guides and 1.06 μm radiation [9].

In addition to self-imaging, Simon and Ulrich [11], suggested that multimode guides with offset inputs and outputs might be used as the basis of fibre optic Mach–Zehnder interferometers. More recently, Pennings et al. [12], have realised this form of interferometer in InGaAsP rib guide technology and have noted a number of potential uses, including: power division, modulation and switching. Soldano et al. [13] have proposed a variant on Simon and Ulrich's [11] design where the input guides have been positioned to limit the set of modes excited in the multimode guide. More sophisticated forms of interferometer based on multimode interference phenomena are also possible. Niemeier and Ulrich [14], have predicted and demonstrated that phase quadrature information can be obtained with interferometers based on 4-to-4-way splitters/mixers with offset input guides. Interferometer designs with multiple input and output arms have been postulated as the basis of N-to-N-way image switches [15]. 1-to-N-way and N-to-N-way optical switches based on fundamental mode input and output guides have also been proposed [16]. 1-to-10-way and 10-to-10-way versions of these devices have recently been demonstrated in GaAs rib guide technology [17].

In our earlier work [8], we noted and demonstrate, that symmetric mode splitters could be used in reverse to recombine or mix fundamental mode input fields. We suggested that such mixers could be the basis of useful interferometers and modulators, in that the result of the mixing process is critically dependent on the relative phases of the fundamental mode input fields. In this paper we apply the concept to the design and demonstration of a novel form of MMI Mach–Zehnder interferometer which has not been previously reported in the literature and which has potential advantages over interferometers described in earlier work. The basic form of the device is illustrated schematically in Fig. 1 in terms of a low loss hollow waveguide structure created in a suitable dielectric substrate. Although the schematic diagram and the theory outlined, specifically relate to hollow guides of the form used in our experimental work, the underlying design concepts are more generally applicable to step index waveguides capable of supporting the required degree of multimode propagation. In suitable semiconductor integrated optic technologies the symmetric MMI interferometer could have considerable potential as an alternative to "Y" junction and evanescent wave based interferometers and modulators.

The interferometer illustrated in Fig. 1 is composed of a symmetric splitter, of the form described earlier [6–10], linked via two mid-way guides, to a symmetric mixer. The mid-way guides act as the arms of the interferometer with optical path differences between them causing changes in the resultant field coupled to the output guides. The interferometer has five distinct waveguide regions: a square input guide, a rectangular splitter guide, two square mid-way guides, a rectangular mixer guide and three square output guides. The structure as illustrated requires a lid which forms the fourth wall of all the guides in question.

The square guides of the structure are all $2a \times 2a$ in cross section, and are capable of supporting fundamental mode propagation. Their length is arbitrary. The two rectangular guides are $2a \times 2b$ in cross section. They are capable of supporting multimode propagation and have a length $L = 2b^2/\lambda$. This value of multimode guide length arises from the more general design criteria for an N-way symmetric splitter, $L_N = (2b)^2/N\lambda_c$, where we chose $N = 2$ for a two-way splitter [6–10]. Here, λ_c is the wavelength of a plane wave in the core of the rectangular guide, i.e. $\lambda_c = \lambda/n$, where n is the refractive index of the core and λ is the vacuum wavelength. For hollow guides, where $n = 1$, $\lambda_c = \lambda$. The single input guide, the two rectangular guides and the centrally located output guide all lie on the same axis whereas the mid-way guides and the two offset output guides are displaced from the axis by $\pm b/2$ respectively. This assumes, as illustrated in Fig. 1, that the sides of the rectangular guide are defined by walls at $-b$ and $+b$, respectively.

The first rectangular guide serves to split the fun-

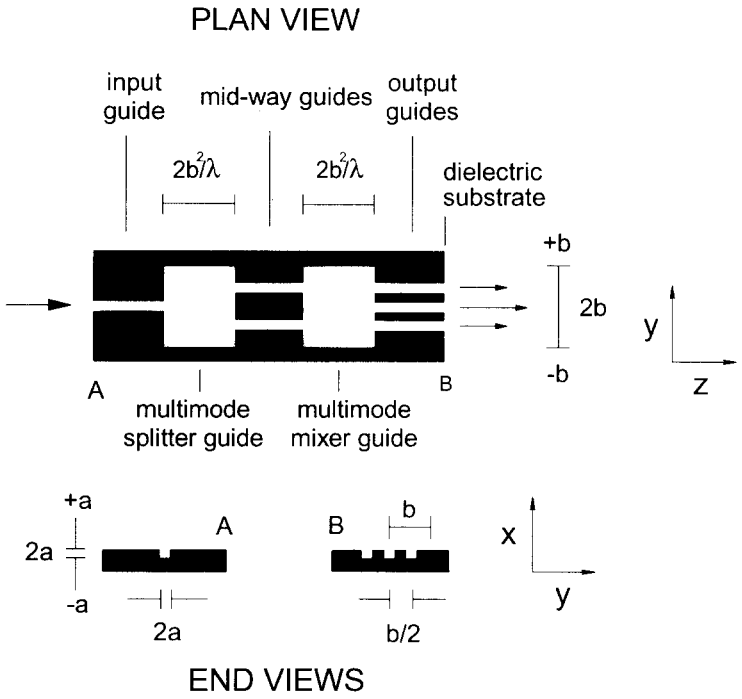

Fig. 1. Schematic diagram of a hollow waveguide MMI Mach-Zehnder interferometer based on the use of a symmetric multimode waveguide splitter and mixer.

damental mode input field equally between the two mid-way guides, whilst the second rectangular guide serves to mix the fields from the mid-way guides and direct the resultant field towards the output guides. The resultant field produced is critically dependent on the relative phases of the fundamental mode fields from the mid-way guides. Although the illustration of the interferometer, and the preceeding description, emphasise the use of three output guides, in a wide variety of applications a single axial output guide should suffice. In such designs, as the rectangular mixer guide only has to accommodate the two mid-way guides, it can be made correspondingly narrower, and, as a result considerably shorter.

In this paper, we describe the underlying theory of the interferometer in terms of the propagation and interference characteristics of the modes of the hollow multimode rectangular waveguides which form the splitter and mixer sections and discuss the details of practical designs. The experiments undertaken with a CO_2 laser source in conjunction with an interferometer based on hollow alumina waveguides are then described. Finally, there is a discussion and conclusion section, where comparisons with earlier published designs are described and concepts for other devices based on multimode interference phenomena are outlined.

2. Mode propagation theory

The multimode propagation characteristics of the rectangular guides of the interferometer are extremely important as far as its performance is concerned. With this in mind we start by reviewing the multimode properties of such waveguides. For the general case of a rectangular cross-sectioned hollow waveguide of height $2a$, and width $2b$, surrounded by a homogeneous dielectric material of complex dielectric constant, ϵ. The normalised linearly polarized EH_{pq} modes, with their time dependency omitted, can be approximately described by the field expression [18,19]:

$$E_{pq}(x, y, z) = (\sqrt{ab})^{-1} \cos(p\pi x/2a) \cos(q\pi y/2b)$$

$$\times \exp(-\gamma_{pq} z), \quad \text{for } p, q \text{ odd},$$
$$= (\sqrt{ab})^{-1} \sin(p\pi x/2a) \sin(q\pi y/2b)$$
$$\times \exp(-\gamma_{pq} z), \quad \text{for } p, q \text{ even}, \qquad (1)$$

where p is the mode number relating to the field dependency along the x-axis, q is the mode number relating to the field dependency along the y-axis, z is the axial variable, and γ_{pq} is the propagation constant of the EH_{pq}th mode; $\gamma_{pq} = \alpha_{pq} - i\beta_{pq}$. Laakmann and Steier [19] give the phase coefficient, β_{pq} of the EH_{pq}th mode as

$$\beta_{pq} = (2\pi/\lambda)\{1 - \tfrac{1}{2}[(p\lambda/4a)^2 + (q\lambda/4b)^2]\}, \qquad (2)$$

where, λ is the vacuum wavelength. It should be noted that the expression predicts that the phase coefficients of the modes are independent of the wall material and is referred to as the "paraxial approximation". Laakmann and Steier [19] also give the attenuation coefficient of the y polarised EH_{pq} mode as

$$\alpha^{y}_{pq} = \frac{\lambda^2 p^2}{16a^3} \operatorname{Re}\left(\frac{1}{(\epsilon - 1)^{1/2}}\right) + \frac{\lambda^2 q^2}{16b^3} \operatorname{Re}\left(\frac{\epsilon}{(\epsilon - 1)^{1/2}}\right)\Bigg]. \qquad (3)$$

Eqs. (1)–(3) are based on two important assumptions: (i) $(4a/p\lambda) \gg 1$, and, $(4b/q\lambda) \gg 1$, (ii) for x-polarised modes, $(4a/p\lambda)(|\epsilon - 1|^{1/2}/\epsilon) \gg 1$, and, $(4b/q\lambda)(|\epsilon - 1|^{1/2}) \gg 1$, and that for y-polarised modes, $(4a/p\lambda)(|\epsilon - 1|^{1/2}) \gg 1$, and $(4b/q\lambda)(|\epsilon - 1|^{1/2}/\epsilon) \gg 1$. The first assumption relates to the fact that the guide cross-section should have dimensions that ensure that the grazing angle between the plane wavelet associated with the EH_{pq}th mode and the wall of the guide is much less than a radian [19]. Under these conditions the second assumption ensures that the wall complex dielectric constant has a value such that the EH_{pq}th mode propagates with low attenuation.

For a given waveguide, where a, b, ϵ and λ are fixed, Eqs. (1)–(3), will only been valid up to a given mode number. This is an important issue. For the multimode splitting and mixing processes to be perfectly achieved the propagating modes must have phase coefficients exactly dictated by Eq. (2). Deviations in the form of the phase coefficients will result in less efficient splitting and mixing, as will any differences in the relative attenuation of the modes in propagating through the splitter and mixer guides. The two effects are clearly linked. In this respect the orders and amplitudes of the modes excited are important variables. Their values will depend upon the geometries of the multimode guides, the positions and numbers of input guides and the nature of the fields which they carry. For the case of a symmetrically fed splitter, i.e. the first stage of the interferometer shown in Fig. 1, Figs. 2a and 2b illustrate how the mode coupling coefficients, relating to mode amplitude $|A_{pq}|$ and intensity $|A_{pq}|^2$, respectively, vary as a function of the ratio of the rectangular guide width, $2b$, to the square input guide width, $2a$, under the assumption that the square input guide carries a fundamental mode field. The plots were generated by numerical calculations of overlap integrals of the form

$$A_{pq_{\text{rec}}} = \int_{-b}^{+b} \int_{-a}^{+a} EH_{11_{\text{squ}}} EH_{pq_{\text{rec}}} \, dy \, dx. \qquad (4)$$

In Eq. (4) the subscripts "rec" and "squ" refer to modes of the rectangular and square guides, respectively. In relation to Figs. 2a and 2b, three points are noteworthy: (i) because of the symmetry of the excitation geometry only the symmetric EH_{pq} modes are excited (i.e. modes with p and q odd); (ii) because the height of the rectangular guide is equal to that of the square guide, when the latter is carrying a funda-

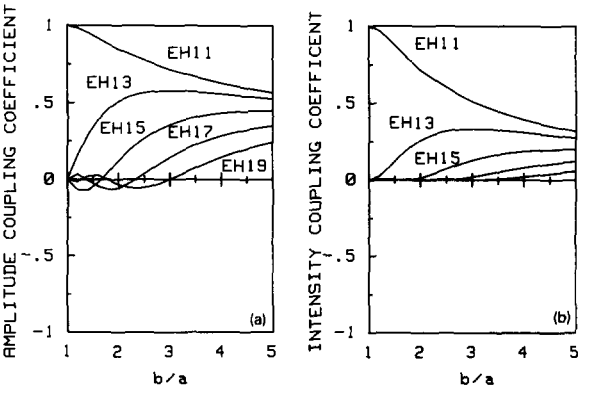

Fig. 2. Mode coupling coefficients: (a) amplitude, $|A_{mn}|$, (b) intensity, $|A_{mn}|^2$, for the splitter section of the interferometer, as a function of the ratio of the rectangular guide width to the square guide width b/a, under the condition that the square cross section input guide is carrying a fundamental mode field.

mental mode field, only the EH_{1q} modes of the rectangular guide are excited – essentially the mode excitation process in the two spatially orthogonal planes is decoupled; (iii) over the range of b/a illustrated, the number of modes excited by the input field is, to a good approximation, directly proportional to the ratio, b/a, e.g. if b/a has an integer value N then first $N+1$ odd modes contain >99% of the fundamental mode input field power (see Fig. 2b).

The minimum rectangular guide width, $2b$, required for an N-way splitter is $2b=N\times 2a$. This creates a useful rule of thumb for the purpose of design and theoretical consideration in that the minimum number of symmetric modes required for an N-way splitter becomes $N+1$. This assumes a zero wall thickness between the output guides. Practical designs might be based on separating the output guides by their own width, i.e. by $2a$. On this basis an N-way splitter would require a rectangular guide width, $2b=2\times N\times 2a$, which would need to support the first, $2N+1$, symmetric modes, the highest order symmetric mode being $EH_{1,4N+1}$.

Figs. 3a and 3b illustrate mode amplitude coupling coefficients $|A_{pq}|$ for the case of a mixer guide (i.e. the second stage of the interferometer) under conditions where the two input guides (the mid-way guides in Fig. 1) are offset from the guide axis by $\pm b/2$, respectively. Figs. 3a and 3b relate to the situation where the fundamental mode input fields are "in" and "out of" phase, respectively. Fig. 3a reveals

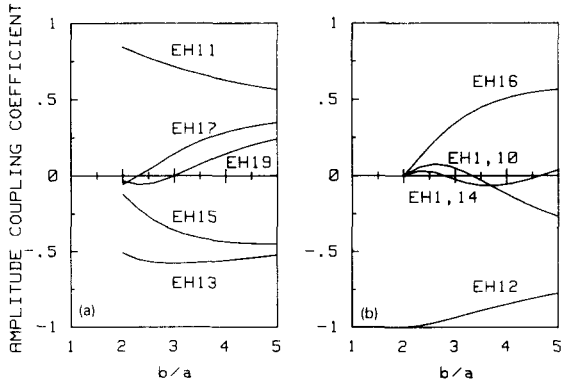

Fig. 3. Mode amplitude coupling coefficients, $|A_{mn}|$, for the mixer section of the interferometer, as a function of the ratio of the rectangular guide width to the square guide width b/a, under the condition that input fields are: (a) "in" phase, (b) "out of" phase.

that, as with Fig. 2a, only the symmetric modes are excited, with the magnitudes of the coupling coefficients in both cases being the same. It should also be noted that some of the coefficients have become negative, with the changes in sign representing the only difference between the mode excitation caused by the two completely different forms of input field. Fig. 3b highlights how a 180° phase shift between the inputs causes only the antisymmetric (even) modes to be excited, i.e. the EH_{1q} modes where q is an even integer. Because of the lateral symmetry of the input guides all the EH_{1q} modes, where $q=i\times 4$, and i is an integer number, remain unexcited.

The establishment of the correct phase relationships between the excited modes at the point $2b^2/\lambda$ along the axes of the rectangular guides is fundamental to the performance of both the splitter and mixer guides. In this respect, the unique nature of the mode dispersion in multimode rectangular waveguides is extremely important. This was first noted by Rivlin and Shul'dyaev [1]. It is useful to predict how the phase difference between two hollow guide modes, EH_{1q} and EH_{1s}, at some point, L, along the guide axis, depends on the guide geometry. As a starting point we will assume that the approximate form of the phase coefficient expression given by Eq. (2) is justified, and establish the practical range of its validity at a latter stage. On this basis we can write the phase difference at the axial point L as

$$\chi_{1q-1s}=L(\beta_{1q}-\beta_{1s})=L(\pi\lambda/16b^2)(s^2-q^2)\,. \qquad (5)$$

For the case of an N-way beam splitter, where $L=(2b)^2/N\lambda$, we can write

$$\chi_{1s-1q}=(\pi/4N)(s^2-q^2)\,. \qquad (6)$$

For a two-way splitter the phase difference between any two modes at the two-way split point simplifies further to: $\pi(s^2-q^2)/8$. As this is a symmetric splitter only the symmetric modes are excited. At this value of L the modes: EH_{13}, EH_{15}, EH_{17}, EH_{19} etc. will have phase differences of: π, 3π, 6π, 10π, etc., with respect to the fundamental. The modes are either "in" phase with the fundamental, as was the case at the guide entrance, or exactly "out of" phase with it. Comparison with Fig. 3a reveals that the ratios and signs of the mode amplitudes are exactly those produced by two "in phase" fundamental mode input fields off set by $\pm b/2$ from the guide axis, respec-

tively. Thus we can conclude that a two-way replication of the fundamental mode input field will be established at this point in good agreement with earlier numerical predictions and experimental results [6–10].

It is possible to extend this form of modal analysis to the recombination of two fundamental mode input fields in the mixer guide. When the inputs are "in" phase, from Fig. 3a, the initial phase offsets of the: EH_{13}, EH_{15}, EH_{17}, and EH_{19} modes, with respect to the fundamental are: π, π, 2π, 2π, etc. Propagation by a further distance $2b^2/\lambda$, results in all modes being brought back in phase with one another, hence reproducing, in agreement with the values predicted in Fig. 2a, a single on-axis fundamental mode field. An analogous argument is possible for the "even", antisymmetric modes, excited in the mixer guide when the fundamental mode inputs are "out of phase". In this case, from Fig. 3b, the lowest order mode is EH_{12}, and its phase differences with respect to the other higher order anti-symmetric modes excited: EH_{16}, $EH_{1,10}$, $EH_{1,14}$, $EH_{1,18}$, etc., following propagation through a distance $2b^2/\lambda$, are all integer multiples of 2π. This once again leads us to conclude that the input field should be regenerated at this guide length, i.e. two, "out of phase" fundamental mode fields offset by $\pm b/2$ from the guide axis should be produced. This condition is also achieved following propagation through b^2/λ.

It is interesting to note that for a similar geometry to the one considered, if we had an N-element input array with a periodic spacing, d, each carrying a fundamental mode field with relative phases alternating between 0 and π, then the array input field would first be reproduced at a distance d^2/λ. This form of periodic reproduction is the waveguide analogue of the Talbot effect [20] which is used extensively as the basis of phase locked resonator designs [21]. For the case where the N fundamental mode inputs from the array were all "in phase" field reproduction would occur at an axial distance of $(Nd)^2/\lambda$.

3. Prediction of transverse field intensity profiles in the splitter and mixer guides

Assuming the use of multimode waveguides where the phase coefficients have a form dictated by Eq. (2) and the attenuation coefficients are very small (and can be taken to be zero), we now predict the transverse field intensity patterns that will occur in the splitter and mixer guides. Figs. 4a–d illustrate calculations of the transverse field intensity and phase at incremental steps of $b^2/3\lambda$ (in terms of integer multiples of λ where $\lambda=\lambda_{11\mathrm{rec}}$) along the axes of the splitter (Fig. 4a) and mixer (Figs. 4b–d) guides where the aspect ratio $b/a=4$. The calculations were based on a transverse field amplitude expression of the form

$$E_z=\sum_{q=1}^{q_{\max}} A_{1q_{\mathrm{rec}}}\,\mathrm{EH}_{1q_{\mathrm{rec}}}\exp(\mathrm{i}\gamma_{1q_{\mathrm{rec}}}z)\,. \tag{7}$$

From the criteria established earlier for the maximum number of modes needed to be supported, we used a value of $q_{\max}=9$. The magnitudes of the complex amplitude coefficients, A_{1q}, of the EH_{1q} modes at, $z=0$, were calculated from overlap integrals of the form given by Eq. (4). The transverse intensity profiles in Figs. 4a–d, were obtained by calculating the square of the modulus of the complex field amplitude from Eq. (7) as a function of y, from $-b$ to $+b$, for $x=0$, i.e. at the half height of the rectangular guide (see Fig. 1).

Fig. 4a indicates that a perfect two-way replication of the fundamental mode input field is formed at a distance of $2b^2/\lambda$, along the guide axis with the replications offset from the axis by $\pm b/2$, respectively.

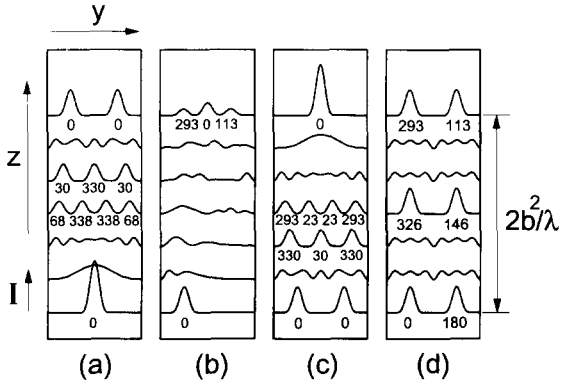

Fig. 4. Predicted transverse field intensity profiles, $I(x=0,y)$ from $-b$ to $+b$, in steps of $b^2/3\lambda$, along the rectangular guide axis, in: (a) the splitter guide with a single symmetrically injected fundamental mode input field, (b) in the mixer guide with a single offset fundamental mode input field, (c) the mixer guide for two offset "in" phase fundamental mode input fields, (c) the mixer guide for two offset "out of" phase fundamental input fields.

Higher order N-way replications can also be observed at axial positions $(2b)^2/N\lambda$ [6–9]. At the replication points the wavefronts are plane. The numbers underneath the replications are the relative phases in degrees, with respect to fundamental mode of the rectangular guide, at the relevant axial points. The phase values have been rounded up to the nearest whole number of degrees as the limited number of modes considered, although adequate in producing intensity profiles of almost perfect fundamental form, result in some small phase errors ($\pm 0.5°$) across each replicated fundamental mode phase front. The N-way replications are symmetric in intensity and phase about the multimode guide axis. The lateral offsets from the guide axis of the components of an N-way replication are given by $y_m = b - (b/N)(2m-1)$, for $m = 1, ..., N$ [8].

Fig. 4b illustrates the resulting field intensity pattern in the mixer guide for a single offset input at $-b/2$. In this case the input field power is divided between the output guides in the ratio 1:2:1. With a single offset input guide at $+b/2$, the relative field intensities in the output guides and the phase of the on axis component would be the same, but the phases of the fields in the two offset output guides will have flipped sides. Figs. 4c and 4d illustrate what happens following the injection of two fundamental mode fields for the two extremes of relative phase difference that can exist between them, i.e. 0° and 180°. When the two inputs are "in" phase (Fig. 4c) they recombine to form a single on axis fundamental mode field, when they are "out of" phase (Fig. 4d) they replicate their input form.

Consideration of the resultant field intensities due to superposition of field output components of the form illustrated in Fig. 4b, for simultaneous input at $-b/2$ and $+b/2$, but with different relative phases established between them, provides an alternative approach to understanding the operation of the interferometer. With two fundamental mode input fields of amplitudes A_1 and A_2, respectively, the intensity profile across the central output guide is given by

$$I(x,y) = \left(\frac{A_1}{\sqrt{2}}\,\mathrm{EH}_{11}(x,y)\right)^2 + \left(\frac{A_2}{\sqrt{2}}\,\mathrm{EH}_{11}(x,y)\right)^2 + 2\,\frac{A_1}{\sqrt{2}}\,\frac{A_2}{\sqrt{2}}\,\mathrm{EH}_{11}^2(x,y)\cos\varphi\,, \tag{8}$$

where $\mathrm{EH}_{11}(x,y)$, is given by Eq. (1) for $z=0$, and φ is the phase difference between the inputs. The power P_{out}, carried in the central output guide is given as

$$P_{\mathrm{out}} = \int_{-a}^{+a}\int_{-a}^{+a} I(x,y)\,\mathrm{d}x\,\mathrm{d}y\,. \tag{9}$$

Assuming the individual fundamental mode input fields with associated amplitudes A_1 and A_2, *each* correspond to an input field power P_{in}, the output power in the central output guide is given as

$$P_{\mathrm{out}} = \frac{P_{\mathrm{in1}}}{2} + \frac{P_{\mathrm{in2}}}{2} + 2\,\frac{\sqrt{P_{\mathrm{in1}}}}{\sqrt{2}}\,\frac{\sqrt{P_{\mathrm{in2}}}}{\sqrt{2}}\cos\varphi\,, \tag{10}$$

where the subscripts "1" and "2" correspond to the individual input guides. From Eq. (10), and supported by Figs. 4c and 4d, it is clear that the power falling onto a detector positioned at the exit of the central output guide would be directly related to the relative phase difference produced between the two mid-way guides. If a phase modulator was integrated into one of these guides this could be used to provide modulation of the power in the on axis output guide.

Assuming the input guides to the mixer were themselves multimode, as could be the case in practice, it is interesting to consider the result of mixing input modes of different order. For example, lets assume that the lefthand input guide to the mixer carried a fundamental mode field of amplitude A_1 whilst the righthand guide carried the mode EH_{13} with an amplitude A_2. From Eq. (8), it is clear that as the phase offset between the inputs changes, corresponding variations in the intensity profile in the central output guide are produced. However, because of the orthogonal nature of the modes, evaluation of the integral in Eq. (9) leads us to conclude that no power variation is produced in the central output guide. Power modulation is only caused as a result of phase changes between like (non-orthogonal) modes propagating in the input guides. This is not a unique characteristic of this form of interferometer. If we consider field mixing in *free space* Mach–Zehnder or Michelson interferometers in terms of the propagation of orthogonal sets of *free space* modes (e.g. as a sets of Hermite–Gaussian modes in a rectangular coordinate system), we come to similar conclusions, i.e. power variations are only produced when the fields

carried in the arms of the interferometers take the form of, individual, or sets of, non-orthogonal modes [#1].

Returning to the waveguide interferometer operating with fundamental mode inputs, from Eq. (10) if the inputs are "in" phase the mixer guide displays "AND" gate characteristics in the manner that the resultant power in the central output guide is dictated by power levels in the input guides. With a power level P_{in} at one of the single offset input guides, a level of $P_{in}/2$ is achieved at the output. With two simultaneous inputs of P_{in}, a power level of $2P_{in}$ is achieved at the output. By modifying the mixer guide geometry in order to derate the output coupling efficiency, for example by making its length $1.7b^2/\lambda$, it is possible to make the resultant outputs for single and double inputs $P_{in}/4$ and P_{in}, respectively. With such a design, a truth table for the case where $P_{in}=1$, would have an end column: 0, 0.25, 0.25, 1. Multiple input "AND" gates could be achieved by concatenation of the basic design element in a suitable semiconductor technology [9]. Multiple input "AND" gates of this form might be useful in realising optical neural networks where phase modulators could be used to provide weighting of the inputs [17]. In this context, it should be noted from Fig. 4c, that with the correct phase offsets, multiple fundamental mode inputs can be recombined to a sole output simply with a multimode mixer guide.

4. Validity of approximations and minimum practical guide cross-sections and lengths

In the discussions and calculations so far, we have assumed that all the excited modes in the splitter and mixer guides propagate with phase coefficients given by Eq. (2) and that they suffer no attenuation in travelling to the axial point, $(2b)^2/2\lambda$. In the limit of very large guide widths compared with the propagating wavelength this situation can always be very closely approached. However, as the required lengths of the splitter and mixer guides scale with the squares of their widths, this can also lead to devices with impractical lengths. If we decided to base a two-way 10.6 μm splitter or mixer on a hollow rectangular guide of width $2b=5.0$ mm, it would need to be $(2b)^2/2\lambda = 117.9$ cm long. Practical designs must be a compromise between minimising the multimode guide width, and hence length, and simultaneously achieving propagation coefficients close to the desired form. Such a design philosophy will mean that the attenuation in the multimode guide might be significant with the result that both phase and amplitude errors will be produced between the excited modes at the point where they couple into the square section output guides. The overall result will be a reduction in the efficiency of the splitter or mixer.

In order to create a sound basis for the design of practically useful interferometers we must calculate the trade offs between multimode guide width, and hence length, and overall efficiency. In order to achieve this goal we start by assessing how the phase and attenuation coefficients in practical waveguides vary with guide width. For the case of a hollow guide with complex dielectric walls we can extend Marcatili's [22] analytical result to give the complex propagation constant for the y-polarised EH_{pq} mode of a rectangular multimode guide as

$$\gamma_{pq}=\left[\gamma-\left(\frac{\pi p}{2a}\right)^2\left(1+\frac{\lambda}{2\pi a(1-\epsilon)}\right)^{-2} -\left(\frac{\pi q}{2b}\right)^2\left(1+\frac{\epsilon\lambda}{2\pi b(1-\epsilon)}\right)^{-2}\right]^{1/2}. \quad (11)$$

The variables are analogous to those used in Eqs. (1)–(3). Assuming that, $2b=4\times(2a)$, and that the complex dielectric constant of the wall at 10.6 μm is given as, $\epsilon=(0.65-i0.135)$ [#2], Eq. (11) was used to calculate values of γ_{pq} as a function of $2b$ for the first five symmetric modes excited in the rectangular splitter guide. These five ($2N+1$ where $N=2$) modes contain 99.35% of the power coupled to the multimode

[#1] In this context it is interesting to note that when such interferometers are used to form coherent radar systems (rangefiders, vibrometers etc) based on the use of fundamental mode (TEM_{00}) lasers, only the fundamental component of the return field can be coherently detected.

[#2] This being the value for the form of polycrystalline alumina (Deranox 975 – a 97.5% pure polycrystalline alumina produced by Morgan Matroc, Surrey, England) that we intended to use in our experiments and whose complex refractive index properties we have measured at 10.59 μm in unpublished work. The stated value is also good agreement with results given by Khelkhal and Herlemont [23] for a 99.9% pure alumina.

guide. The fractional powers carried by each mode ($EH_{11}-EH_{19}$) are: 0.39, 0.31, 0.19, 0.08 and 0.02, respectively. These correspond to fractional amplitudes of: 0.63, 0.56, 0.43, 0.29, and 0.15. In conjunction with these amplitudes the respective values of γ_{pq} were used to predict the field at the limit of the rectangular splitter guide and the efficiency with which it would couple to fundamental mode fields in the two square section output guides. Values of $2b$ of: 1.6 mm, 1.2 mm, 0.8 mm and 0.4 mm, yielded total fundamental mode power coupling coefficients of: 0.9447, 0.9288, 0.9003 and 0.8230, respectively.

Non-unity fundamental mode power coupling coefficients can result for two reasons. Firstly, propagation along the multimode guide to the point of entry into the square cross section guides results in attenuation. Secondly, any changes in the relative amplitudes of the modes caused by this attenuation, and any phase changes brought about by modal dispersion not of a form dictated by Eq. (2), will result in imperfections in the field replication process. In turn this results in a reduction in the efficiency with which fundamental fields are excited in the output guides. Our calculations revealed that the biggest influence on the fundamental mode coupling efficiency was the attenuation in the multimode guide. Fractional power transmissions of: 0.9448, 0.9296, 0.9014 and 0.8242 were predicted for the four different guide widths. Consideration of the differences between the two sets of figures leads to the conclusion that the phase and amplitude errors had little impact on efficiency.

For completeness, with the phase error established between the EH_{11} and EH_{19} modes defined as

$$\chi=\frac{(2b)^2}{2\lambda}\{[\beta_{19}\text{Eq.}(2)-\beta_{11}\text{Eq.}(2)] - [\beta_{19}\text{Eq.}(11)-\beta_{19}\text{Eq.}(11)]\}, \quad (12)$$

we calculated values for χ of: 3.1°, 4.3°, 5.0° and 5.7° for the four multimode guide widths. We also calculated that propagation through the guide results in the relative amplitudes of the EH_{11} and EH_{19} modes being reduced by the following factors: (EH_{11}/EH_{19}), 0.98/0.97, 0.97/0.96, 0.96/0.94 and 0.93/0.79. The much smaller reduction in efficiency caused by the phase and amplitude errors is related to the small relative changes produced between the excited modes.

We concluded from these calculations that with predicted power splitting/mixing efficiencies of $\approx 95\%$, hollow alumina guides of width $2b=1.6$ mm and length 121 mm would be practical both as splitters and mixers. Scaling from the rectangular guide width, the square cross-section input, mid-way and output guides would need to be 0.4 mm in width. With $2b=4\times 2a$ only a single discrete axial output guide is possible from the mixer. The square guide dimensions are very large compared with the propagating wavelength with the result that they will not be single mode guides. However, with careful lateral and angular alignment of a TEM_{00} input field, as proved in earlier work [8], efficient excitation of the fundamental mode can be achieved. In practice measurements suggest that in excess of 95% of the power carried in the TEM_{00} input field can be coupled to the fundamental waveguide mode. A design close to the one described above was used as the basis of the experimental work which is described in the following section.

5. Experiment work and results

The hollow waveguide version of the MMI Mach–Zehnder interferometer was proved experimentally with a combination of hollow alumina waveguides and hollow core silica fibres in conjunction with a 10.6 μm CO_2 laser source. The experimental configuration is illustrated in Fig. 5. Two hollow rectangular guides acted as the splitter and mixer regions, these being interconnected by two hollow core silica fibres which acted as the mid-way guides, i.e. the arms of the interferometer. There were no input or output guides of the form indicated in Fig. 1, instead, the TEM_{00} laser field was coupled directly into the first splitter guide and the field output from the mixer guide was observed directly. This had the advantage that the true form of the output field could be observed without it being filtered by single mode output guides or fibres.

Each rectangular guide was fabricated from four pieces of polycrystalline alumina, two which were "T" shaped in cross section, and two which were square in cross section. When formed, the hollow rectangular guides were each 0.75 ± 0.05 mm high, 1.5 ± 0.05 mm wide and 212.0 ± 1.0 mm in length. From the de-

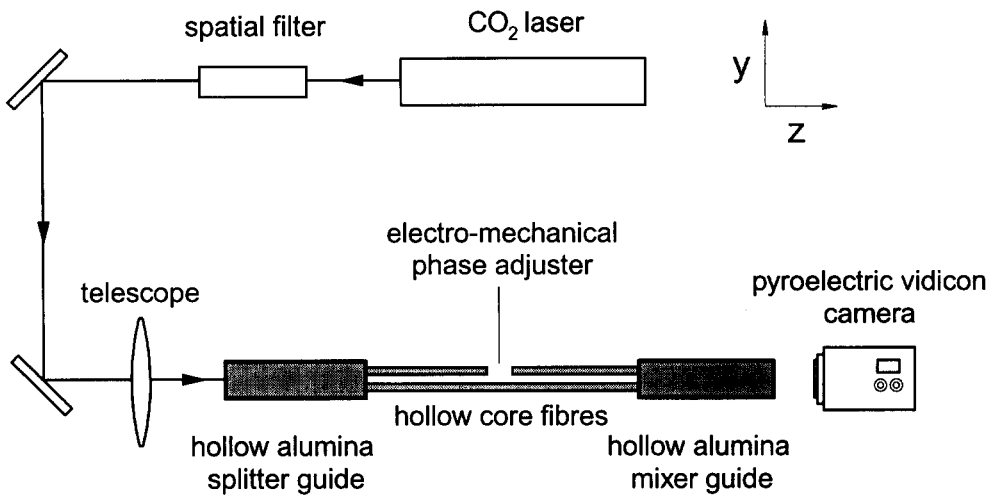

Fig. 5. Schematic diagram of the experimental configuration, highlighting the use of hollow core fibres and hollow core rectangular waveguides in the practical demonstration of the MMI Mach–Zehnder interferometer. The phase adjuster works by accurately varying the separation between the mid-way brake in the fibre, hence changing its overall optical path length.

sign expression, $L=(2b)^2/2\lambda$, the required active length of the rectangular splitter and mixer guides for 10.6 μm operation is, 106 mm. The additional 106 mm length present in both the splitter and mixer guides was used for fibre guidance purposes. The guide cross sections were designed to provided a good fit for the pair of 40 cm long 0.70 ± 0.05 mm OD, 0.50 ± 0.05 mm ID, hollow core silica fibres.

The characteristics of the fibres had been studied experimentally in unpublished work. Although they exhibited a large attenuation coefficient even when held straight (≈ 10 dB/m), their fundamental mode fidelity was very good even with 50 cm radii of curvature bends. Although the fibres are multimode, any higher order mode excitation appeared to be completely suppressed as a result of the much greater attenuation of the higher order modes compared with the fundamental. As a consequence no problems were anticipated with regard to the fidelity of the fundamental mode beams entering the mixer guide as a result of fibre curvature or of input field misalignment from the splitter.

A means of achieving phase offsets between the outputs of the two fibres on entry to the mixer guide was established as follows. One of the two fibres was cut into two half lengths, each half then being approximately 20 cm long. The "cut ends" were carefully clamped in "fixed" and "computer controlled" stepper motor mounts. The computer controlled mount, allowed both accurate alignment of the fibre ends with respect to one other, and their accurate axial separation. In this manner, the relative phase between the fields entering the mixer guide from the two fibres, could be varied in steps of $\sim 36°$ ($\equiv 1.0$ μm path difference), with accuracies of $\sim 9°$ ($\equiv 0.25$ μm path difference). Having set up the electro-mechanical phase modulator as described, the ends of the fibres were accurately positioned in the splitter and mixer guides, respectively.

The resulting configuration deviated a little from the proposed design in that the rectangular guide width was only a factor of three larger than the fibre ID whilst its height was somewhat greater than the fibre ID. In the splitter this should result in a reduction in the efficiency with which the replicated input field can be coupled to fundamental mode fields in the fibres. In addition these modifications have two different effects on the performance of the mixer. The former would result in both a reduction in the physical separation of the lobes of the resultant "out" of phase output pattern, and in a small reduction in the degree of higher order mode excitation in the horizontal plane of the multimode guide. Conversely, the latter deviation should result in an increase in the higher order mode excitation in the vertical plane of the mixer guide, e.g. some excitation of the EH_{3q} and

EH_{5q} modes should occur. This is associated with the fact that smaller dimensioned fundamental mode fields will be injected into the mixer guide than had been originally predicted. However, with the waveguide having a height $2a = 0.75$ mm, the active length of 106 mm equates to $2 \times (2a)^2/N\lambda$, where $N = 1$. As far as the vertical component of the field is concerned this guide length is double that which would produced input field regeneration [8,10]. As a consequence the overall effect of the deviations from the proposed design should be small distortions of the output field patterns compared with those predicted in Figs. 4c and 4d, and a slight increase in attenuation in both the splitter and mixer guides.

The experimental measurements were based on the use of a CO_2 laser which was grating tuned to give an output on the P20/10 transition at 10.59 μm. This was checked on an optical spectrum analyser. With an optogalvanic stabilisation system in operation the laser had a long term (tens of minutes) frequency stability of better than ±5 MHz, i.e. a wavelength stability of $\pm 1.9 \times 10^{-6}$ μm. Following spatial filtering, which ensured a high fidelity TEM_{00} beam ($\geq 95\%$ power in TEM_{00}), the horizontally polarised output was projected into a telescope which was arranged to produce a well aligned beam of waist, $w = 0.7a$, at the splitter guide entrance. This choice of beam waist led to an input field which was a very good approximation to the fundamental mode field from a $2a \times 2a$ square guide ($\approx 98\%$ of the energy in a TEM_{00} beam of this waist size would be coupled into the fundamental mode of a guide $2a$ square [19]).

The general goal of the alignment procedures was to make the input beam and the axis of the rectangular splitter guide coaxial. With this situation closely achieved, a pyroelectric vidicon camera was used to directly study the output profile at a distance of 10 cm from the mixer guide. This allowed more accurate alignment to be established. Once this process was completed, the output field from the mixer guide was recorded as a function of the relative optical path difference between the two fibres. Figs. 6 and 7 illustrate the two normalised (peak power equalized) extremes of the measured output profile in terms of 2D intensity contour, and 1D intensity profile, plots. The coordinate system utilized in these figures is commensurate with that used in Figs. 1 and 4. Owing to limitations in the gray scales available for the contour illustration, pure "white" was used to represent both the lowest and highest powers, i.e. the background and the peak power, respectively. The true form of the transverse nature of the intensity profiles is clarified by the 1D intensity profiles. These correspond to positions represented by the horizontal lines across the contour plots.

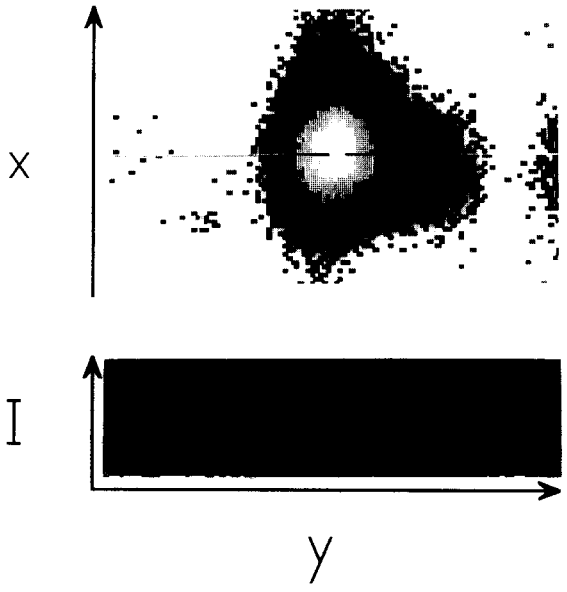

Fig. 6. One extreme of the measured output intensity profile from the mixer guide, in 2D contour and 1D profile form (corresponding to the position indicated by the horizontal line across the contour plot), correlating well with the "in" phase field intensity prediction in Fig. 4c.

Fig. 6 illustrates a single on-axis output field of quasi-gaussian form in good agreement with the field predictions of Fig. 4c for the case where the mixer guide input fields are "in phase". Conversely, Fig. 7 shows two offset lobes, each of quasi-gaussian form, in good agreement with Fig. 4d, under the condition where the inputs to the mixer guide are "out of" phase. Both sets of profiles show some slight elongation along the x axis. In separate experiments the power transmission of the mixer guide under both extremes of input phase was measured as $87 \pm 0.5\%$. Although the absolute phase difference between the input fields to the mixer guide could not be ascertained, a change in the axial separation of the "halved" fibre ends of ~ 5.0 μm caused the resultant intensity pattern to change from one extreme to the other, confirming the theoretical predictions. In

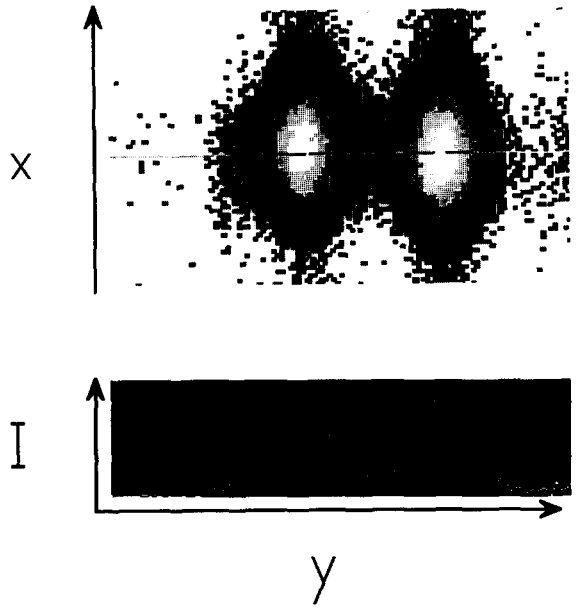

Fig. 7. The other extreme of the measure output intensity profile from the mixer guide, in 2D contour and 1D profile form (corresponding to the position by the horizontal line across the contour plot), brought about by $a \approx 5.3$ μm change in the optical path length of the fibre compared with that needed to achieve the profile in Fig. 6 and correlating well with the "out of" phase field intensity prediction in Fig. 4d.

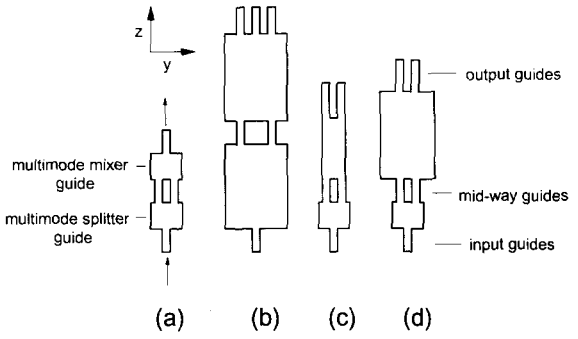

Fig. 8. Comparison of geometries (plan views) for four potential MMI interferometer/modulator designs all with symmetric 1-to-2-way MMI splitters as the input stage and with recombiner/mixer stages as described in: (a) and (b) this paper, (c) by Simon and Ulrich [11] and Pennings et al. [12], and, (d) by Soldano et al. [13]. All have square cross section fundamental mode, input, mid-way and output guides, and, rectangular cross section multimode, splitter and mixer guides.

comparison with the theory both the elongation of the output field profiles, and the slightly higher than predicted attenuation, are explicable in terms of the modifications to the theoretical design and diffraction effects.

6. Comparisons of MMI Interferometer designs

MMI interferometers should have a number of applications in a wide range of step index waveguide technologies, both as sensors, and in conjunction with suitable phase transducers, as intensity modulators. In terms of such applications a comparison with other forms of multimode interferometer that can be conceived, in terms of their functionality and design is worth while. Some of the possibilities are illustrated in Figs. 8a–d. All are assumed to be based on input, midway and output guides of width 2a, with spacing such that their outer walls are separated from one another by 2a. All are assume to have symmetric input splitters to achieve a two-way split of the source [6–10]. Figs. 8a and 8b, illustrate the interferometer described in this paper with, one and three output guides, respectively. We refer to them as "symmetric" interferometers, because they always produce resultant output fields which are symmetric about the mixer guide axis. Figs. 8c and 8d illustrate asymmetric interferometers with mixer sections postulated by Simon and Ulrich [11] (and demonstrated by Pennings et al. [12]) and by Soldano et al. [13], respectively. In both these designs there are two output guides and the resultant field swings between them. The axial separation of the midway and output guides in design 8c are arbitrary whereas those in 8d must be positioned at $\pm b/3$, in order to suppress excitation of the $EH_{1,q\times 3}$ modes, where q is and integer number.

Figs. 9a–d illustrate the resultant field patterns in the mixer sections of designs 8c and 8d under conditions where the phase offsets between the inputs are chosen to produce the two extremes of the output field patterns in each. The axial separations between the intensity profiles are shown in terms of the multimode guide half width b. Figs. 9a and 9b relate to design 8c and highlight how single fundamental mode field output patterns are produced at the left and right output guides of the mixer section for input phases (from left to right) of 0° and 90°, and 0° and 270°, respectively. Figs. 9c and 9d relate to the design 8d, this performs in a similar way to design 8c but for a

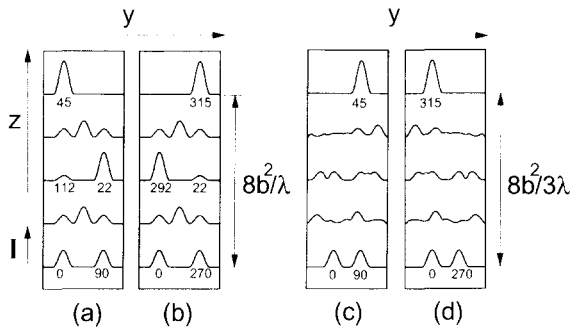

Fig. 9. Predicted transverse field intensity profiles, $I(x=0, y)$, from $-b$ to $+b$, for the designs illustrated in Figs. 8c and 8d. Figs. 9a and 9b relate to design 8c whilst Figs. 9c and 9d relate to design 8d. The figures show the resultant field intensities in each of the two designs for the two extremes of input phase difference.

given set of input phases the output intensity profiles have flipped sides.

Bearing in mind our design criteria for input and output guide separation, we now consider the geometric trades offs between the different designs. The single output guide version of the symmetric interferometer, illustrated in Fig. 8a, requires a rectangular guide width, $2b=4(2a)$, and a length $L=(2b)^2/2\lambda = 8(2a)^2/\lambda$. The three output guide version illustrated in Fig. 8b, requires a rectangular guide width of $8(2a)$, and a mixer guide length $L=32(2a)^2/\lambda$. In this design the width and hence length of the splitter guide also has to be scaled in order to form a complete interferometer. In design 8c, as long as the input and output guides are symmetrically offset from the mixer guide axis, the magnitude of the offset is arbitrary. In order to minimise the rectangular guide width we can chose, $2b=3(2a)$, and position the input and output guide axes at $\pm 2a$ from the rectangular guide axes as Pennings et al. [12] have suggested. With this design the required mixer guide length is given as $L=(4b)^2/2\lambda=18(2a)^2$. In the design illustrated in Fig. 8d the mixer guide has to have a length of $2(2b)^2/3\lambda$. In this design the input and output guide axes have to have a separation $4a$, however, this also has to equate to one third of the rectangular guide width. As a result we need to make $2b=6(2a)$, the required mixer guide length then becomes, $24(2a)^2/\lambda$.

From these considerations, the mixer stage of the "single output guide" version of the "symmetric mode" interferometer, illustrated in Fig. 8a, is less than half the length of all the other designs. However, designs 8c and 8d are useful as variable beam splitters or as balanced mixers where signal to noise reduction operations could be performed. In this case Simon and Ulrich's [11] design is a little shorter than that proposed by Soldano et al. [13], and considerably shorter than the "three output guide" version of the symmetric interferometer design.

From Figs. 9a and 9b, a further design based on the field patterns formed at the mid-way point $4b^2/\lambda$, can be considered. Although the minima is finite, rather than zero, the fact that the multimode guide length can be halved will be attractive for devices based on lossy waveguides. It should be appreciated that the transverse field patterns produced at the axial point $2b^2/\lambda$ in Figs. 9a and 9b, for input phases, from left to right, of 0° and 90°, and 0° and 270°, respectively, are the mid-cycle points between the phase offset extremes of Figs. 4c and 4d. Starting from the fundamental mode output field in Figs. 9a or 9b counter propagation by a distance of $4b^2/\lambda$ highlights a potentially useful asymmetric splitter with a ratio of $\sim 6:1$ [24]. As a consequence the $4b^2/\lambda$ design also has potential as a bi-directional coupler.

Although symmetric 1-to-2-way splitters are advocated as the basis of the input stages to all the interferometers shown in Fig. 8 the use of more than one input creates interesting possibilities. Simon and Ulrich [11] have suggested an interferometer design with a 2-to-2-way splitter of length $2(2b)^2/\lambda$ as the input stage and with a mixer of the same length. As there are two possible input positions either could be switched to either output. Simon and Ulrich [11] hinted at extending this concept to devices with larger numbers of input and output ports whilst Ulrich [15] has suggested designs which can facilitate N-to-N-way image switching. We have proposed designs where symmetric 1-to-N-way splitters of length $(2b)^2/N\lambda$ or offset splitters of length $4(2b)^2/N\lambda$ are coupled via fundamental mode mid-way guides incorporating electro-optic phase transducers to N-to-N-way recombiners of length $4(2b)^2/N\lambda$ [16]. We have shown that such designs allow point to multi-point as well as point to point switching and have recently demonstrated 1-to-10-way and 10-to-10-way devices in GaAs rib guide technology [17].

7. Discussions and conclusions

In this paper a novel form of a Mach–Zehnder interferometer has been postulated and demonstrated based on multimode interference phenomena in rectangular multimode waveguides. In the limit, the multimode guides only need to support the first half-dozen or so higher order waveguide modes. In a wide range of waveguide technologies, this form of interferometer could form the basis of sensors and intensity modulators. In semiconductor technologies the interferometer could be important for OEICs whilst in its hollow waveguide format it could be a basis for gas sensors and spectrometers where the gas to be studied was flowed through, or allowed to permeate into, the midway guides. In conjunction with a suitable phase modulator, integration of the interferometer into a laser cavity could provide a novel means of providing Q-switching and "cavity dumping" functions.

Current work is aimed at proving the underlying interferometer concepts in semiconductor, step index, waveguide technologies and extending the concepts to 1-to-N-way and N-to-N-way optical routing devices. The significantly lower attenuation coefficients achievable with waveguides based on total internal reflection phenomena allow the design of splitters and mixers based on input and output guides of a few wavelengths in width. This in turn leads to a pro-rata reduction in the width and length of the multimode guide required for a given order of splitting. We have demonstrated a 1-to-20-way splitter in GaAs rib guide technology based on fundamental mode input and output guides of 2.6 μm in width, where the multimode guide was 120 μm wide and 2.37 mm long [9]. On this basis we could create interferometers of an analogous design to the one described, where the splitter and mixer guides were 10 μm wide and less than 200 μm in length [#3].

The realisation of the growing range of device functions made possible by multimode interference phenomena, in the right integrated optic technologies, could form the basis of a new generation of integrated optic devices and provide scope for new architectures for OEICs and for I.O. optical computing and optical signal processing systems. Although the potential in semiconductor I.O. technologies is very important, the broad applicability of the underlying concepts, in terms of both waveguide technology, and operating wavelength, are also worth noting. The symmetric mode splitters are and excellent example of this point, where the underlying concepts have been proved at 10.6 μm, with millimeter cross section, hollow guides, of centimeters in length, and at 1.06 μm, with GaAs rib guides of tens of μm in width and hundreds of μm in length [6–10].

[#3] In an analogous manner to our studies of MMI splitters [6–9], since the work described in this paper was undertaken, the concepts have also been successfully proved in GaAs rib guide technology [25].

Acknowledgements

The authors are indebted to Dr. G. Brown, Dr. A. Scott and Dr. D. Wight, for their continued support and encouragement. Mike Jenkins would like to thank the following people for useful discussions: (i) Dr. P.K. Milsom, DRA, Malvern, Worcestershire, (ii) Dr. A.R. Davies and Dr. J. Banerji, RHC, University of London, Egham, Surrey, (iii) Dr. D. Wheatley, Laser Ecosse, Dundee, Scotland.

References

[1] L.A. Rivlin and V.S. Shul'dyaev, Radiophys. Quantum Electron. 11 (1968) 318.
[2] O. Bryngdahl, J. Opt. Soc. Am. 63 (1973) 416.
[3] R. Ulrich, Optics Comm. 13 (1975) 259.
[4] R. Ulrich and G. Ankele, Appl. Phys. Lett. 27 (1973) 337.
[5] R.M. Jenkins and R.W.J. Devereux, Appl. Optics 31 (1992) 5086.
[6] R.M. Jenkins and J.M. Heaton, International patent application no. PCT/GB91/02129, filed December 2nd, 1991, U.K. patent priority date, December 20th, 1990.
[7] R.M. Jenkins and R.W.J. Devereux, International patent application no. PCT/GB91/02132, filed December 2nd, 1991, U.K. patent priority date, December 20th, 1990.
[8] R.M. Jenkins, R.W.J. Devereux and J.M. Heaton, Optics Lett. 17 (1992) 991.
[9] J.M. Heaton, R.M. Jenkins, D.R. Wight, J.T. Parker, J.C.H. Birbeck and K.P. Hilton, Appl. Phys. Lett. 61 (1992) 1754.
[10] R.M. Jenkins, R.W.J. Devereux and J.M. Heaton, Field regeneration, splitting and recombination in multimode waveguides, IEEE Quantum Electron. submitted.
[11] A. Simon and R. Ulrich, Appl. Phys. Lett. 31 (1977) 77.

[12] E.C.M. Pennings, R.J. Deri, A. Scherer, R. Bhat, T.R. Hayes, N.C. Andreadakis, M.K. Smit, L.B. Soldano and R.J. Hawkins, Appl. Phys. Lett. 59 (1991) 1926.
[13] L.B. Soldano, F.B. Veerman, M.K. Smit, B.H. Verbeek, and E.C.M. Pennings, in: Digest of Conf. Integrated Photonics Research (Opt. Soc. Am., Washington, 1991) paper ThF1, p. 107.
[14] Th. Niemeier and R. Ulrich, Optics Lett. 11 (1960) 677.
[15] R. Ulrich, U.K. patent application no. 1 525 492, 1978.
[16] R.M. Jenkins and J.M. Heaton, International patent application no. PCT/GB91/02130, filed December 2nd, 1991, U.K. patent priority date, December 20th, 1990.
[17] R.M. Jenkins, J.M. Heaton, D.R. Wight, J.T. Parker, J.C.H. Birbeck, G.W. Smith and K.P. Hilton, Appl. Phys. Lett. 64 (1994) 684.
[18] H. Krammer, IEEE J. Quantum Electron. QE-12 (1976) 505.
[19] K.D. Laakmann and W.H. Steier, Appl. Optics 15 (1976) 1334.
[20] H.F. Talbot, Philos. Mag. J. Sci. 9 (1936) 401.
[21] M. Jansen, J.J. Yang, S.S. Ou, D. Botez, J. Wilcox and L. Mawse, Appl. Phys. Lett. 55 (1989) 1949.
[22] E.A.J. Marcatili, Bell System Technical Journal, Sept (1969) 2071.
[23] Khelkhal and Herlemont, Appl. Optics 31 (1992) 4175.
[24] R.M. Jenkins, International patent application no. PCT/GB91/02131, filed December 2nd, 1991, U.K. patent priority date, December 20th, 1990.
[25] J.M. Heaton, R.M. Jenkins, D.R. Wight, J.T. Parker, J.C.H. Birbeck and K.P. Hilton, Multiway beam splitters and recombiners using self-imaging properties of multimode GaAs/AlGaAs waveguides, presented at Semiconductor and Integrated Opto-Electronics, SIOE'93, Cardiff, Wales, March, 1993.